

Emissions related to donor-bound excitons in highly purified zinc selenide single crystals

著者	須藤 彰三
journal or publication title	Physical review. B
volume	36
number	5
page range	2568-2577
year	1987
URL	http://hdl.handle.net/10097/35426

doi: 10.1103/PhysRevB.36.2568

Emissions related to donor-bound excitons in highly purified zinc selenide single crystals

M. Isshiki, T. Kyotani, and K. Masumoto

Department of Materials Science, Faculty of Engineering, Tohoku University, Sendai 980, Japan

W. Uchida and S. Suto

Physics Department, College of General Education, Tohoku University, Sendai 980, Japan

(Received 20 January 1987)

Photoluminescence (PL), selective photoluminescence, and photoluminescence excitation (PLE) spectra have been measured on high-purity ZnSe single crystals at 4.2 K. Zn-dip treatment at 973 K for a week makes the I_1^f line disappear and the effective temperature of free-exciton gas decrease from 8.4 to 5.6 K through an increase in the lifetime of the free excitons. Accurate agreement is found for the transition energies of donor-bound excitons and their excited states with the values reported by Dean *et al.* Accurate values are estimated for the effective-mass donor binding energy and the static dielectric constant. The notable spectral feature in the PL spectra is that the emission intensities of the I_3 lines are higher than those of the I_2 lines. The origin of I_3 , the recombination of the excitons bound to ionized donors, is considered to be unreliable, judging from the donor-concentration dependence of the intensity ratio between the I_2 and I_3 emission lines and the spectral change under a cw dye-laser excitation with the energy below the band gap. PLE spectra show that the peaks related to excited states of I_2 exist in the PLE spectra for I_3 in addition to the other peaks related to the excited states of I_3 , and that the spectra for I_{3s} is similar to that for I_{3w} .

I. INTRODUCTION

Zinc selenide is one of the most promising materials for fabricating a blue-light-emitting device with high efficiency. Few successful techniques have been developed for growing low-resistivity *p*-type crystals. For the preparation of a low-resistivity crystal, high-purity ZnSe single crystals with extremely low donor concentration should be grown and then the doping effect of acceptor-type impurities should be examined. From this point of view, high-purity zinc selenide single crystals have been grown^{1,2} using commercial-grade high-purity selenium and zinc purified by vacuum distillation and overlap zone melting³ in our laboratory.

Photoluminescence (PL) spectra have been widely used by many authors for qualitative evaluation of the purity (especially, donor concentrations) of their ZnSe crystals. Donors contribute to PL in the near-band-gap region in various ways. The detected luminescence due to the resulting transitions are very useful for the characterization of chemical species of donors contained in the crystals and donor states. In this case accurate values should exist for the transition energies of donor-bound excitons and their excited states. However, the transition energies previously reported are scattered.

Detailed studies of PL on ZnSe were first performed by Merz *et al.*⁴ They determined the transition energies of no-phonon donor-bound excitons and their excited states and also donor binding energies and their excited levels. On the other hand, Dean *et al.*⁵ reported about 0.25-meV uniformly higher transition energies for the donor-bound excitons. This energy displacement is too large to assign the emission lines in measured PL spectra.

For the estimation of donor binding energies using a

hydrogenic model, the value of the effective-mass binding energy (E_D^0) is very important. The reported values of E_D^0 are 28.8 meV (Ref. 4) and 26.06 meV (Ref. 5). Furthermore, the reported value of the static dielectric constant (ϵ_s) used for the estimation of E_D^0 is widely scattered from 8.66 (Ref. 4) or 8.8 (Ref. 6) to 9.14 (Ref. 5). The present paper determines accurate energy values mentioned above in ZnSe from the analysis of photoluminescence (PL), selective photoluminescence (SPL), and photoluminescence excitation (PLE) spectra measured on high-purity ZnSe single crystals grown by a vapor-phase transport technique.^{1,2}

In the previous papers on the evaluation of grown crystals through PL measurements,² it was found that the emission due to the recombination of free excitons (RFE) is much stronger than those of I_2 and I_3 , and the peak energy of RFE emission is lowered by the Zn-dip treatment. This change of RFE peak energy was explained by considering the increase of the free-exciton lifetime. The notable spectral feature observed is that the emission intensities of I_3 lines are larger than those of I_2 lines. This phenomenon is quite different from the previous results expected as the origin of I_3 emission is a radiative recombination of excitons bound to ionized donors.⁴

In the present paper the more-detailed discussions are given on emissions of RFE and donor-bound excitons. The discussions are also given on the excited states of donor-bound excitons (I_2 and I_3) estimated from the PLE spectra measured using a cw dye laser.

II. EXPERIMENTAL PROCEDURE

Zinc selenide polycrystal was synthesized at 1273 K in a vacuum-sealed quartz ampoule using purified zinc.^{1,2}

and commercial selenium of 99.999% purity (Mitsubishi Metal Co.). The synthesized polycrystals were refined by sublimation method, and ZnSe single crystals were grown by vapor-phase transport using a Zn reservoir⁷ and a special shape growth chamber.⁸ Temperatures of the source and crystallization chambers were kept at 1283 and 1278 K, respectively. Zn-dip treatment was performed at 973 K for a week in a vacuum-sealed quartz ampoule.

Samples for PL measurement were prepared by cleaving the grown single crystals and etched at 363 K using a solution consisting of three parts saturated aqueous solution (at 333 K) of $K_2Cr_2O_7$ and two parts concentrated H_2SO_4 . The photoluminescence spectra were measured at 4.2 K using a double monochromator having a resolution of 0.06 meV, and ultraviolet light from a 2-kW Xe lamp as the excitation source.

For the measurement of the PLE and SPL spectra, a cw dye laser pumped by the uv lines of a Kr^{+} -ion laser was used as the excitation source. The output power is controlled at a constant value, about 10 mW, as the wavelength is tuned continuously from 420 to 450 nm with the use of stilbene-3 dye. The value of the full width at half maximum (FWHM) of the excitation light from the dye laser was 0.3 meV.

III. EXPERIMENTAL RESULTS

A. Photoluminescence

Photoluminescence spectrum measured on as-grown crystal is shown in Fig. 1(a). It should be noted that the emission intensities of donor-bound excitons are remarkably small and the emission intensity of the radiative recombinations of free excitons (RFE) is very strong. This fact indicates that the purity of the grown crystal is very high and that the donor concentration in this crystal is very low. Furthermore, LO-phonon replicas of free excitons (ex), ex-LO, and ex-2LO, are clearly observed.

After the Zn-dip treatment, the PL spectrum changes as shown in Fig. 1(b). The noteworthy spectral features

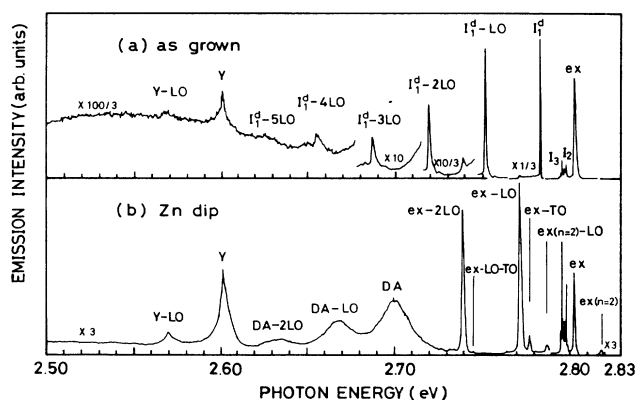


FIG. 1. Photoluminescence spectra measured on (a) as-grown ZnSe single crystal and (b) the crystal Zn-dip treated at 973 K for a week. The emission due to radiative RFE has been labeled "ex."

are that the I_1^d line disappears, and the intensities of intrinsic emissions related to free excitons, ex-LO, ex-2LO, ex-TO, ex-(LO+TO), ex($n=2$), and ex($n=2$)-LO, remarkably increase, where TO and ex($n=2$) represent TO phonon and the emission of radiative recombination of free excitons in an excited state ($n=2$), respectively. The emission intensity of ex-3LO is estimated to be negligibly small although the emission cannot be detected because of the superposition with the $D-A$ pair emission. The emission intensities of I_2 and I_3 relatively increase compared with those on the as-grown crystal. This increase is known to be caused not by a contamination but by the increase in the lifetime of the free excitons due to the decrease of free-exciton trapping by zinc vacancies,³ and by the increase in the isolated donor concentration due to the decrease of donor- V_{Zn} associated defect concentration resulting from Zn-dip treatment.⁹

Other spectra changes caused by the Zn-dip treatment are that the broad band around 2.5–2.6 eV detected on the as-grown crystal disappears and the $D-A$ pair emission band with its phonon replicas appears after the Zn-dip treatment. In the present paper no discussion about Y emission and $D-A$ pair emission will be given.

Figure 2 shows the PL spectra in the donor-bound exciton region. Assignment of each emission line is performed by reference to Merz *et al.*⁴ and Dean *et al.*⁵ Their peak energies are tabulated in Table I. The values of transition energies obtained in the present work are in good agreement with those reported by Dean *et al.*, while the values by Merz *et al.* are uniformly 0.25 meV lower than the present values as pointed out by Dean *et al.*⁵ It should be noted that the Zn-dip treatment decreases the peak energy of RFE by about 0.2 meV. This means that the lifetime of free excitons increases through the vanishing of zinc vacancies as a scattering center for the free excitons. Actually, the I_1^d line, which is strongly detected on the as-grown crystal, disappears after the Zn-dip treatment.

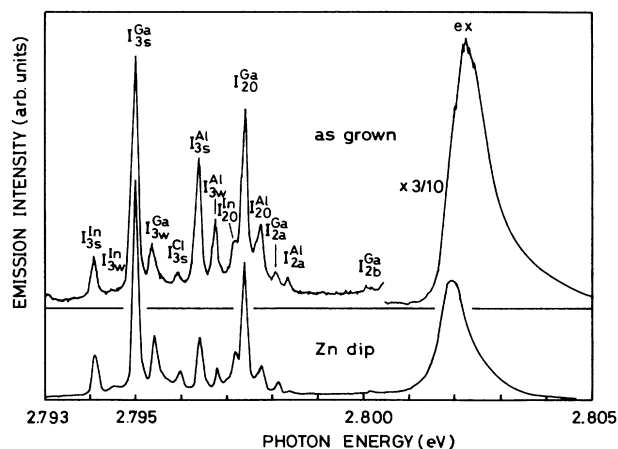


FIG. 2. PL spectra in donor-bound-exciton region measured on the ZnSe single crystals before and after Zn-dip treatment. Note that the emission intensities of I_3 are larger than those of I_2 and the peak energy of RFE lowers after Zn-dip treatment.

TABLE I. Transition energies of various bound-exciton no-phonon components. Reported values are also shown. The peak energies of five unknown emissions T_1 – T_5 are also listed. Transition energy of I_{20}^{Cl} is obtained by the excitation spectrum of I_{3s}^{Cl} in the present paper.

Component	Transition energy (eV)		
	Merz <i>et al.</i> ^a	Dean <i>et al.</i> ^b	Present work
I_{20}^{Al}	2.797 54	2.7977 ₆	2.797 77
I_{20}^{Cl}	2.797 45	2.7977 ₀	2.797 74
I_{20}^{Ga}	2.797 18	2.7975 ₁	2.797 42
I_{20}^{In}	2.796 97	2.7972 ₂	2.797 21
I_{20}^{F}	2.796 9	2.7970 ₅	
I_{3w}^{Al}	2.796 53		2.796 79
I_{3s}^{Al}	2.796 15		2.796 41
I_3^{Cl}		2.7965 ₅	
I_{3w}^{Cl}	2.796 14	2.7963 ₈	
I_{3s}^{Cl}	2.795 74	2.7959 ₈	2.795 98
I_{3w}^{Ga}	2.795 18		2.795 43
I_{3s}^{Ga}	2.794 77		2.795 02
I_{3w}^{In}	2.794 29	2.7945 ₂	2.794 56
I_{3s}^{In}	2.793 88	2.7941 ₃	2.794 13
I_{3s}^{F}	2.793 88		
I_{3w}^{F}	2.793 48		
T_1			2.793 15
T_2			2.792 60
T_3			2.792 31
T_4			2.781 79
T_5			2.775 46

^aReference 4.

^bReference 5.

The spectral feature of particular note is that the emission intensities of I_3 lines are larger than those of I_2 lines. This phenomenon is quite different from the results previously reported.

B. Selective photoluminescence

Selective photoluminescence spectra were measured under the excitation at the energies of each I_2 and I_3 emission line. Figures 3 and 4 are the spectra measured in the energy region just below the excitation energy and in that of the two-electron transition, respectively. The I_3 lines of Al, Ga, and In are detected in Fig. 3. Five unknown emissions labeled T_1 to T_5 are seen in the figures. The peak energy of these emission lines are listed in Table I.

The emissions due to the two-electron-transition process are clearly observed in Fig. 4 by tuning the excitation energy to the energy of I_{20}^{Ga} and I_{20}^{Al} , while the excitations at the energy of I_3 do not show any additional emission peak related to the two-electron transition. The results of SPL spectra on other I_3 lines are similar to those of I_{3w}^{Al} and I_{3s}^{Al} . It should be noted that the emissions due to the two-electron transitions to 3s and 3p excited states are clearly observed in addition to those to 2s and 2p excited states. Dean *et al.*⁵ also detected two-electron transitions to 3s and 3p on In and Ga. In the case of Al, this is the first observation on two-electron transitions to the 3s and 3p states. The spectra detected in the present experiments are more clear than those reported by Dean *et al.*⁵

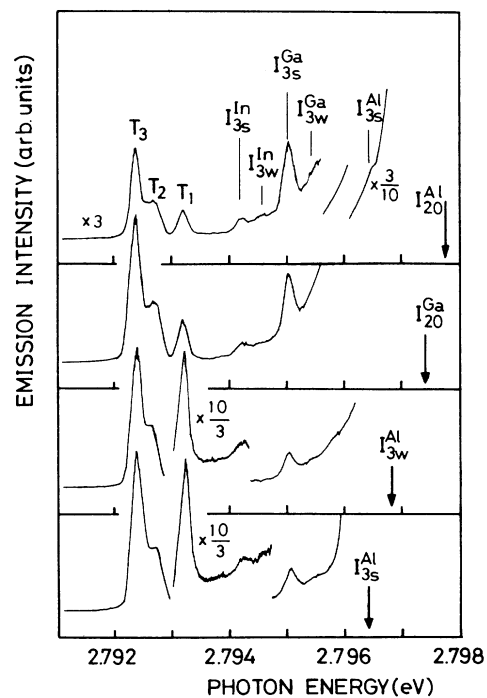


FIG. 3. Selective photoluminescence spectra. Arrows indicate the excitation energy to which the dye laser is tuned. T_1 , T_2 , and T_3 are unknown emission lines.

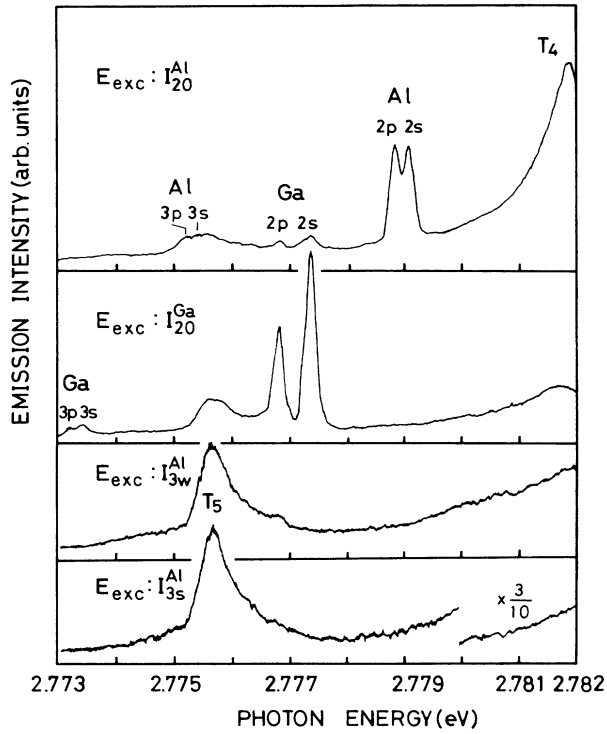


FIG. 4. Selective photoluminescence spectra in two-electron transition regions. E_{exc} denotes the excitation energy. The emissions due to two electron transition to $3s$ and $3p$ donor excited states as well as those to $2s$ and $2p$ excited states are clearly observed, in the case that the excitation energy is tuned to I_{20} emission lines. Two broad emission lines, T_4 and T_5 , are unknown emission lines.

C. Photoluminescence excitation spectra

Figure 5 shows the PLE spectra of I_{20}^{Al} and I_{20}^{Ga} . In both cases, sharp $I_{2\alpha}$ peaks ($\alpha = a, b, c, d,$ and e) reported by Dean *et al.*,⁵ and $I_{2\beta}$ and $I_{2\beta'}$ reported by Kasuya *et al.*,¹⁰ are clearly seen. Among the $I_{2\alpha}$ peaks, the peak

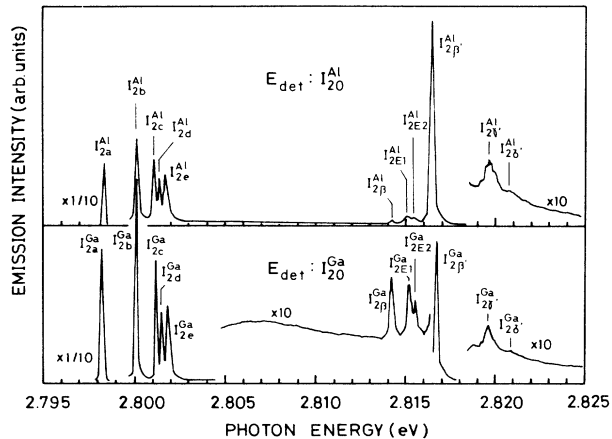


FIG. 5. Photoluminescence excitation spectra of I_{20}^{Al} and I_{20}^{Ga} . E_{det} denotes the fixed detection energy.

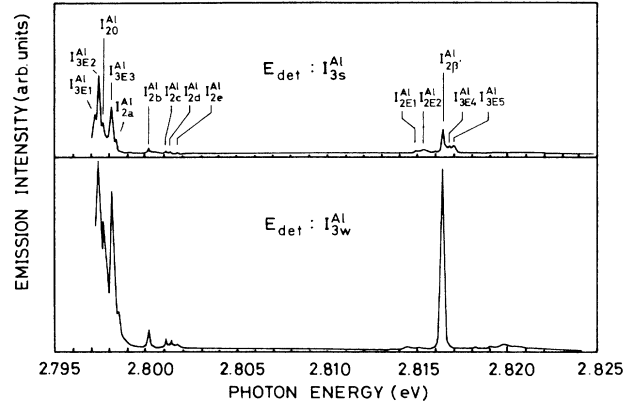


FIG. 6. Photoluminescence excitation spectra of I_{3s}^{Al} and I_{3w}^{Al} .

of I_{2e}^{Ga} is the first observation in the present experiment. Between $I_{2\beta}$ and $I_{2\beta'}$, two broad peaks labeled I_{2E1} and I_{2E2} are found in both cases of Al and Ga. Furthermore, two broad peaks, $I_{2\gamma'}$ and $I_{2\delta'}$, are also found in the energy region higher than $I_{2\beta'}$. The peak energies detected in Fig. 5 are listed in Table II together with those previously reported.

Photoluminescence excitation spectra on I_{3s}^{Al} and I_{3w}^{Al} are shown in Fig. 6. It is found that both spectra are similar to that of I_{20}^{Al} , although the spectra have the additional structure labeled I_{3E1} – I_{3E5} . The spectral feature in the low-energy region is that there are five $I_{2\alpha}$ peaks, I_{20}^{Al} and new peaks labeled I_{3E1}^{Al} , I_{3E2}^{Al} , and I_{3E3}^{Al} . The peak energies of $I_{2\alpha}^{Al}$ and I_{20}^{Al} detected in these spectra are in good agreement with the values listed in Table I within experimental error (0.06 meV), although the peak intensities of $I_{2\alpha}^{Al}$ and I_{20}^{Al} are relatively low compared with the PLE spectrum on I_{20}^{Al} .

In the case of the PLE spectra of I_{3s}^{Ga} and I_{3w}^{Ga} shown in Fig. 7, the peak intensities of $I_{2\alpha}^{Ga}$ are weak and rather broad and that of I_{20}^{Ga} is strong compared with those of I_{3E1}^{Ga} and I_{3E2}^{Ga} . The assignment of the detected peaks is

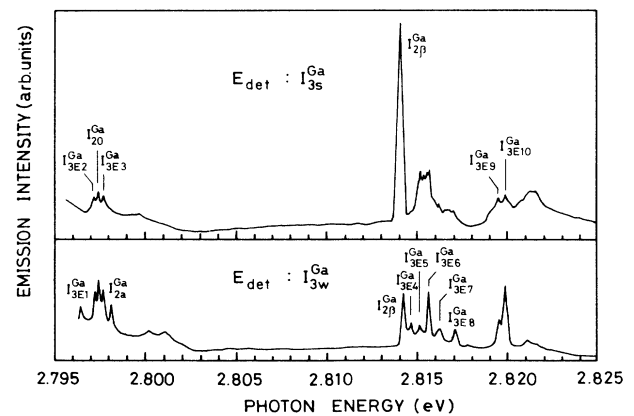


FIG. 7. Photoluminescence excitation spectra of I_{3s}^{Ga} and I_{3w}^{Ga} .

TABLE II. Transition energies of excited states of I_{20} , obtained from excitation spectra. In the cases of Cl and In, the transition energies are obtained from their excitation spectra on I_{3S} .

Component	Transition energy (eV)			
	Merz <i>et al.</i> ^a	Dean <i>et al.</i> ^b	Kasuya <i>et al.</i> ^c	Present
I_{2a}^{Al}	2.798 16	2.7983 ₉		2.798 41
I_{2b}^{Al}	2.799 99	2.8002 ₁		2.800 23
I_{2c}^{Al}	2.800 90	2.8011 ₁		2.801 07
I_{2d}^{Al}	2.801 18	2.8013 ₈		2.801 35
I_{2e}^{Al}		2.8017 ₂		2.801 73
$I_{2\beta}^{Al}$			2.814 45	2.814 29
I_{2E1}^{Al}				2.815 01
I_{2E2}^{Al}				2.815 43
$I_{2\beta'}^{Al}$			2.816 70	2.816 53
$I_{2\gamma'}^{Al}$				2.819 73
$I_{2\delta'}^{Al}$				2.820 81
I_{2a}^{Cl}	2.798 10	2.7983 ₆		2.798 42
I_{2b}^{Cl}	2.799 98	2.8002 ₃		2.800 20
I_{2c}^{Cl}	2.800 90			2.801 18
I_{2d}^{Cl}	2.801 19			2.801 46
I_{2e}^{Cl}				2.801 82
$I_{2\beta}^{Cl}$			2.814 40	2.814 23
$I_{2\beta'}^{Cl}$			2.816 82	2.816 75
I_{2a}^{Ga}	2.797 90	2.7982 ₃		2.798 24
I_{2b}^{Ga}	2.799 92	2.8002 ₄		2.800 22
I_{2c}^{Ga}	2.800 91	2.8012 ₃		2.801 23
I_{2d}^{Ga}	2.801 19	2.8015 ₁		2.801 53
I_{2e}^{Ga}				2.801 90
$I_{2\beta}^{Ga}$			2.814 30	2.814 24
I_{2E1}^{Ga}				2.815 15
I_{2E2}^{Ga}				2.815 65
$I_{2\beta'}^{Ga}$			2.817 01	2.816 82
$I_{2\gamma'}^{Ga}$				2.819 77
$I_{2\delta'}^{Ga}$				2.820 96
I_{2a}^{In}	2.797 79	2.7980 ₅		
I_{2b}^{In}	2.799 83	2.8001 ₀		
I_{2c}^{In}	2.800 85			
I_{2d}^{In}	2.801 13	2.8014 ₀		
$I_{2\beta}^{In}$			2.814 28	2.814 21
$I_{2\beta'}^{In}$			2.817 12	2.816 92

^aReference 4.

^bReference 5.

^cReference 10.

performed by referring to their peak energies, although I_{3E3}^{Ga} should be exchanged by I_{20}^{Ga} , taking into consideration the similarity of the PLE spectra between I_{3S}^{Al} and I_{3W}^{Ga} in the lower-energy region. On the other hand, the structure in the higher-energy region is stronger and sharper than those of I_{3S}^{Al} and I_{3W}^{Al} . The difference of the PLE spectra between I_3 peaks of Al and Ga shows the dependence of PLE spectra on I_3 upon donor chemical species. The tendency is made clearer by the comparison with the PLE spectra on I_{3S}^{Cl} and I_{3S}^{In} shown in Fig. 8. There should exist a trend that the donor element with the lower mass number gives the higher peak intensities in the lower-energy region. The trend is reversed in the high-energy region.

The transition energies detected in the PLE spectra of I_3 are listed in Table III.

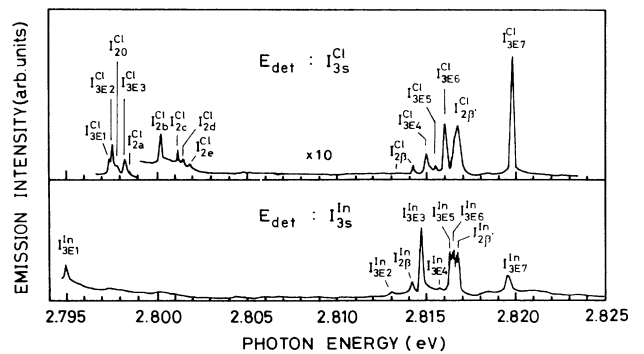


FIG. 8. Photoluminescence excitation spectra of I_{3S}^{Cl} and I_{3S}^{In} .

TABLE III. Transition energies of I_3 excited states.

Component	Transition energy (eV)
I_{3E1}^{Al}	2.797 23
I_{3E2}^{Al}	2.797 42
I_{3E3}^{Al}	2.798 15
I_{3E4}^{Al}	2.816 83
I_{3E5}^{Al}	2.817 07
I_{3E1}^{Cl}	2.797 30
I_{3E2}^{Cl}	2.797 48
I_{3E3}^{Cl}	2.798 13
I_{3E4}^{Cl}	2.814 96
I_{3E5}^{Cl}	2.815 46
I_{3E6}^{Cl}	2.816 06
I_{3E7}^{Cl}	2.819 88
I_{3E1}^{Ga}	2.796 46
I_{3E2}^{Ga}	2.797 29
I_{3E3}^{Ga}	2.797 72
I_{3E4}^{Ga}	2.814 59
I_{3E5}^{Ga}	2.815 06
I_{3E6}^{Ga}	2.815 59
I_{3E7}^{Ga}	2.816 32
I_{3E8}^{Ga}	2.817 06
I_{3E9}^{Ga}	2.819 53
I_{3E10}^{Ga}	2.819 93
I_{3E1}^{In}	2.719 46
I_{3E2}^{In}	2.812 98
I_{3E3}^{In}	2.814 75
I_{3E4}^{In}	2.815 67
I_{3E5}^{In}	2.816 36
I_{3E6}^{In}	2.816 60
I_{3E7}^{In}	2.819 78

IV. DISCUSSION

A. Emissions related to free excitons

Comparing the PL spectra shown in Fig. 1, the I_1^d line disappears and the emission related to free excitons becomes strong after the Zn-dip treatment. Huang *et al.*¹¹ suggested from their ingenious experiments that there exist two origins for I_1^d emission, Cu_{Zn} and V_{Zn} . It is considered that the origin of I_1^d observed in the present experiment on the as-grown crystal is V_{Zn} . Zn-dip treatment decreases the concentration of V_{Zn} as a scattering center for free excitons. Consequently, the lifetime of the free excitons increases.

If the lifetime of the free excitons increases, the effective temperature of the free-exciton gas will decrease and then the distribution of the free exciton, on the excitonic polariton dispersion, will shift towards the lower-energy side as the wave vector of the excitonic polariton decreases. Actually, the peak energy of the RFE is lowered by about 0.2 meV after the Zn-dip treatment as shown in Fig. 2. The effective temperatures of free-exciton gas are estimated from their RFE emission line to make the situation more clear.

Using the effective temperature of the free excitons, T_f , the shape of the zero-phonon free-exciton luminescence

line, $F(E)$, is expressed¹² by

$$F(E) \sim E^{1/2} \exp(-E/kT_f), \quad (1)$$

where $E = E_i - E_0$ is the kinetic energy of the excitons in a band with bottom energy E_0 . The first factor in Eq. (1) is the density of states in the parabolic exciton band, neglecting some minor corrections caused by the excitonic polariton dispersion. With use of Eq. (1), the effective temperature is estimated from the slope of the relation between $\ln[F(E)E^{-1/2}]$ and E . T_f values of 8.4 and 5.6 K are obtained in the RFE emission lines measured before and after the Zn-dip treatment from the linear relations shown in Fig. 9. This fact indicates directly the increase in the lifetime of the free excitons. It should be noted that the effective temperature of free-exciton gas is close to the lattice temperature, in the case of the Zn-dip-treated crystal.

The spectral feature in RFE lines shown in Fig. 2 is that the excitonic polariton effect do not appear. Usually, the RFE line from the upper polariton branch is observed as a shoulder of emission line from the lower polariton branch. The RFE line observed in the present experiment is thought to be all from the lower polariton branch. The increase in the lifetime of the free excitons causes the transition of the excitonic polariton from the upper to the lower polariton branch through an acoustic-phonon-assisted process. The straight lines obtained in Fig. 9 are proof of this deduction. If the emission of the upper polariton branch exists, there should appear a hump near about 2 meV of E on the plots of Fig. 9.

B. Donor binding energy

As mentioned in Sec. III B, the emissions due to two-electron transitions to $3s$ and $3p$ excited states on Al and Ga donors, as well as those to $2s$ and $2p$ excited states, are clearly seen in Fig. 4. Dean *et al.*⁵ found those to $3s$ and $3p$ excited states on Ga and In donors. The energy displacements between the tuned excitation energy and the emission peaks due to two-electron transitions of each donor are given in Table IV together with those reported previously. It is known that the values obtained in the present experiment are consistent with those reported previously.

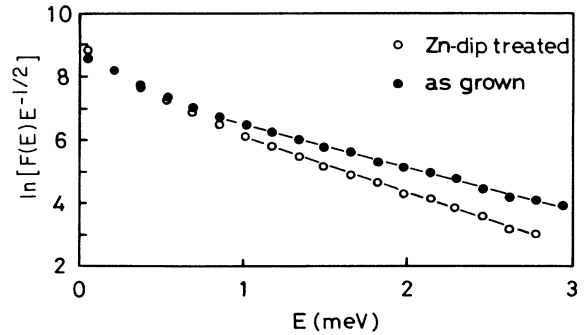


FIG. 9. Relation between $\ln[F(E)E^{-1/2}]$ and E . The resulting plots show linear relationships, the slope being $(kT_f)^{-1}$.

TABLE IV. Donor excitation energies and donor binding energies.

Donor	Reference	Excitation energy (meV)				Binding energy (meV)	
		$2s - 1s$	$2p - 1s$	$3s - 1s$	$3p - 1s$	E_D^*	E_D^{**}
Al	Present work	18.91	19.14	22.59	22.75	25.66 ^a 26.95 ^b	25.65 ^a 26.34 ^b
	Dean <i>et al.</i> ^c	18.84	19.12				25.64 ^a
	Merz <i>et al.</i> ^d	18.87	19.14				26.3 ^b
	Kasuya <i>et al.</i> ^e	18.91	19.16				
Cl	Dean <i>et al.</i> ^c	19.36	19.67				26.19 ^a
	Merz <i>et al.</i> ^d	19.35	19.66				26.9 ^b
	Kasuya <i>et al.</i> ^e	19.32	19.71				
Ga	Present work	20.16	20.72	24.18	24.37	27.27 ^a 27.57 ^b	27.24 ^a 27.91 ^b
	Dean <i>et al.</i> ^c	20.18	20.71	24.13	24.33		27.23 ^a
	Merz <i>et al.</i> ^d	20.22	20.72				27.9 ^b
	Kasuya <i>et al.</i> ^e	20.18	20.78				
In	Present work	20.92	21.71				28.23 ^a
	Dean <i>et al.</i> ^c	20.91	21.68	25.03	25.32		28.20 ^a
	Merz <i>et al.</i> ^d	20.89	21.70				28.9 ^b
	Kasuya <i>et al.</i> ^e	20.90	21.75				

^aCalculated with $E_D^0 = 26.06$.

^bCalculated with $E_D^0 = 28.8$.

^cReference 5.

^dReference 4.

^eReference 10.

Dean *et al.*⁵ suggested that the energy difference between $2p$ and $3p$ donor states should deduce the value of the effective-mass donor binding energy E_D^0 of 26.06 ± 0.15 meV, which is significantly smaller than the value reported by Merz *et al.*,⁴ $E_D^0 = 28.8 \pm 2.4$ meV. Consequently, the values of donor binding energy E_D reported by Merz *et al.*⁴ are higher than those by Dean *et al.*, since E_D is assessed from adding the binding energy of the $2p$ state of $E_D^0/4$ to the measured energy difference of $E(2p - 1s)$ (E_D values obtained in this way are represented as E_D^{**} in Table IV). The value of E_D can be also estimated in the form of $E_D^* = E(3p - 1s) + E_D^0/9$. Taking into consideration the central cell effect, E_D^* can be considered to be reliable rather than E_D^{**} . If the value of E_D^0 is accurate, the calculated values of E_D^* should be equal to that of E_D^{**} . As shown in Table IV, the values of E_D^* are in good agreement with those of E_D^{**} in the case of $E_D^0 = 26.06$. This fact supports the suggestion by Dean *et al.*,⁵ except there is insistence on the dielectric constant.

Effective-mass donor binding energy is calculated using the relationship

$$E_D^0 = (m_e^*/\epsilon_s^2)E_h, \quad (2)$$

where E_h , m_e^* , and ϵ_s are the binding energy of the hydrogen atom, the electron effective mass, and the dielectric constant, respectively. The values of m_e^* and ϵ_s used for calculating values of E_D^0 are listed in Table V. Merz *et al.*⁴ and Dean *et al.*⁵ obtained $0.16m$ for m_e^* from their own experiments on the Zeeman effect. Merz

et al. estimated the value of E_D^0 as 28.8 meV with reference to the unpublished value 8.66 for ϵ_s . On the other hand, Dean *et al.* insisted, from their m_e^* value and E_D^0 estimated from the energy difference between $2p$ and $3p$ donor states, that the value of ϵ_s should be 9.14. Recently, Ohyama *et al.*¹³ obtained $0.145m$ for a m_e^* value from their first cyclotron resonance study on ZnSe. Using this value of m_e^* and 26.06 of E_D^0 , we can obtain 8.70 for ϵ_s , which is very close to the value of 8.66 by Roberts and Marple cited by Merz *et al.*⁴

Neumark⁶ estimated the value of ϵ_s as 8.8 from a detailed analysis of pair spectra measured on Na-doped ZnSe crystals and the obtained value of ϵ_s is close to the value estimated in the present paper. Neumark *et al.*¹⁴ estimated, however, the E_D^0 as 28 meV using $m_e^* = 0.16m$ and $\epsilon_s = 8.8$. We can conclude that the reliable values of m_e^* , ϵ_s , and E_D^0 are $0.145m$ (Ref. 13), 8.70, and 26.06 (Ref. 5), respectively. Consequently, the reliable

TABLE V. The values of m_e^* and ϵ_s for the calculation of the effective-mass donor binding energy E_D^0 .

Authors	m_e^*	ϵ_s	E_D^0
Merz <i>et al.</i> ^a	0.16	8.66	28.8
Dean <i>et al.</i> ^b	0.16	9.14	26.0 ₆
Present work	0.145	8.70	26.06

^aReference 4.

^bReference 5.

values of the donor binding energy of ZnSe are those reported by Dean *et al.*⁵

C. Luminescence of I_3

As mentioned in Sec. III A, a noteworthy spectral feature in the donor-bound-exciton emission spectra shown in Fig. 3 is the inversion of the emission intensities between I_2 and I_3 compared with the reported spectra measured on the ZnSe crystals. The intensity ratio is found to be dependent on the purity of the crystals, especially on the donor concentration N_D . Figure 10 indicates the dependence of the emission intensity ratio I_3/I_2 on the emission intensity of I_2 line normalized by that of each RFE line. The value of $I_2/I(\text{ex})$ is not proportional to N_D , but is a function of N_D . It is obvious that the decrease in N_D causes a relative increase in the emission intensity of I_3 by more than 2 orders.

Donor species in ZnSe crystal are, in general, substantially compensated at equilibrium. However, they have a very large cross section for the capture of free electrons at low temperatures due to their Coulomb attraction potential. This means that a large portion of donors should be photoneutralized under continuous photoexcitation with the energy higher than the E_g of ZnSe as adopted in the present experiments.

Considering the recombination process of the photoexcited free carriers, the main process for producing ionized donors is considered to be $D-A$ pair recombination. The lower concentration of impurities gives the larger displacement between donor and acceptor in the crystal. This means that the photoneutralized donors in the higher-purity crystals have a longer lifetime compared with those in less-pure crystals. This consideration is inconsistent

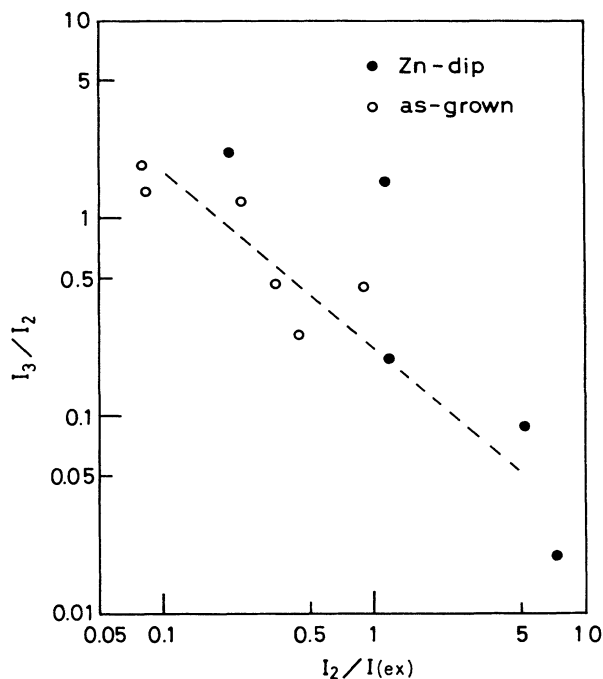


FIG. 10. Relation between the emission intensity ratio I_3/I_2 and the emission intensity of I_2 normalized to that of RFE.

with the donor concentration dependence of the emission intensity ratio between I_2 and I_3 shown in Fig. 10.

Dean *et al.*⁵ suggested that the free holes produced through the photoexcitation could increase ionized donors by capturing at neutral donors nonradiatively. However, their suggestion cannot explain our result, because the probability of free holes at neutral donors should not change by more than 2 orders through the changes of N_D and N_A . If the ionization of the photoneutralized donors is caused mainly by the capture of free holes, the emission intensity ratio between I_2 and I_3 will be dependent on the intensity of the excitation light. Such a dependence is not observed in the present experiment, though the excitation intensity is changed by 2 orders in additional experiments.

To make the situation more clear, the PL spectrum was measured under the excitation by the light from a cw dye laser with the energy of 2.811 eV, where there is no excited state of donor-bound excitons as shown in Fig. 5–8. Excitation of 2.811 eV, lower than E_g , creates only free excitons of the $n=1$ state with appropriate kinetic energy. In this case, free carriers seldom are created and photoneutralization does not occur. If the origin of the I_3 emission is the ionized donor, it would be expected, under such an excitation, that the emission intensities of I_3 lines should increase relatively and the emission intensity ratio between I_2 and I_3 should settle down at a value determined by a compensation ratio of the specimen. Figure 11 shows the spectrum measured under such a condition. It is clear that the intensities of the I_3 lines are rather lower compared with the spectra shown in Fig. 2.

As mentioned above, all the results obtained in the present experiments are contrary to the results expected as the origin of the I_3 emissions is the radiative recombination of the excitons bound to ionized donor as proposed by Merz *et al.*⁴ Recently, the temperature dependence of the electron relaxation time was reported by Ohyama *et al.*¹⁵ from the linewidth broadening of the cyclotron resonance absorption of photoexcited electrons. Their result does not show any contribution of ionized impurity scattering under the photoexcitation

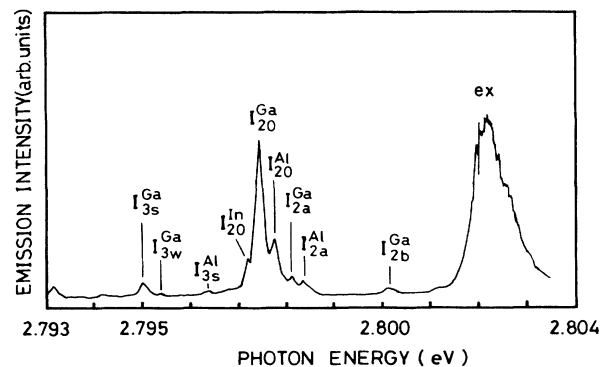


FIG. 11. Photoluminescence spectrum measured under the excitation using the light from the dye laser with the energy tuned to 2.811 eV. Note that the intensities of I_3 emission lines remarkably decrease compared with the spectra shown in Fig. 2, which are measured under the excitation with the energy higher than band-gap energy.

with the energy higher than E_g . This means directly the absence of the nonradiative hole capture at photoneutralized donors.

The chemical species of each donor-bound-exciton line in the spectra in Fig. 2 are consistent with the result obtained by Merz *et al.*,⁴ because it is found that the usage of crystals of different concentrations of only aluminum causes the change of relative emission intensities related to only aluminum, I_{20}^{Al} , I_{3s}^{Al} , I_{3w}^{Al} , and I_{2a}^{Al} without change in these relative intensities. Furthermore, the selective excitation spectra excited at each donor-bound-exciton line are also consistent with the results by Merz *et al.*⁴ These results indicate that the contradictions to the origin of I_3 emission, mentioned in the present paper, might not be caused by the misapprehension as the emissions due to isoelectronic trap of nitrogen in GaP were assigned to I_3 emission.¹⁶

Unfortunately, detailed Zeeman-effect measurements on I_3 lines have not been made in the case of ZnSe. Further experimental and theoretical investigations must be done to make the situation more clear.

D. Excited states of I_2 and I_3

Dean *et al.*⁵ and Kasuya *et al.*¹⁰ reported the excited spectra of I_2 lines using cw tunable dye lasers. As shown in Fig. 5, five $I_{2\alpha}$ peaks are clearly detected on each donor. These results are consistent with the results by Dean *et al.*⁵ On the other hand, $I_{2\beta}$ and $I_{2\beta'}$ peaks are also clearly observed as reported by Kasuya *et al.*

Kasuya *et al.*¹⁰ assigned $I_{2\beta}$ and $I_{2\beta'}$ to the states of the excited donor-bound exciton denoted as (X_{2s}, D_{1s}) and (X_{1s}, D_{2s}) , respectively, where X_{1s} and D_{1s} indicate the excitons and neutral donors at ground state, respectively, and the subscript $2s$ shows that there exist at the $2s$ excited state. The energy locations of $I_{2\beta}$ and $I_{2\beta'}$ can be expressed as

$$E(I_{2\beta}) \sim E(I_{20}) + [E(X_{2s}) - E(X_{1s})] \quad (3)$$

and

$$E(I_{2\beta'}) \sim E(I_{20}) + [E(D_{2s}) - E(D_{1s})], \quad (4)$$

where $E(X_{ns})$ and $E(D_{ns})$ are the energy levels of exciton and donor at the ns excited state, respectively. Although the chemical shifts exist up to 1.86 meV for each donor, the calculated values agree well with the energies of $I_{2\beta}$ and $I_{2\beta'}$.¹⁰

By an analogy with the above discussion, the origins of $I_{2\gamma'}$ and $I_{2\delta'}$ can be considered to be related to higher excited states of donor-bound excitons. The calculated values of higher excited states for Al and Ga are shown in Table VI. The energies of (X_{3s}, D_{1s}) and (X_{4s}, D_{1s}) are calculated from the binding energy of exciton $E_B = 19$ meV,¹⁷ assuming Rydberg series for $3s$ and $4s$ exciton levels. The energies of (X_{1s}, D_{3s}) are directly obtained from the measured values of $E(3s - 1s)$ listed in Table IV. For estimating the values of $E(4s - 1s)$, it is assumed that the $4s$ donor levels are obtained by adding the energy differences between $E_D(n=4)$ and $E_D(n=3)$ of the effective-mass donor to those of $E(3p - 1s)$. Permitting the chemical-shift values slightly larger than those existing in the case of $I_{2\beta}$ and $I_{2\beta'}$, it can be de-

TABLE VI. Calculated transition energies of the higher excited states of neutral donor-bound excitons for Al, Ga, and In donors.

Excited state	Al	Ga	In
(X_{3s}, D_{1s})	2.814 66	2.814 31	2.814 10
(X_{4s}, D_{1s})	2.815 58	2.815 23	2.815 02
(X_{1s}, D_{3s})	2.820 36	2.821 60	2.822 24
(X_{1s}, D_{4s})	2.821 79	2.823 04	2.823 80

duced that $I_{2\gamma'}$ and $I_{2\delta'}$ originate in (X_{1s}, D_{3s}) and (X_{1s}, D_{4s}) , respectively. Using these models, the broadening of these peaks can be explained due to narrower discrete energy levels in the excited states of $n > 3$.

Between $I_{2\beta}$ and $I_{2\beta'}$, there exist two peaks labeled I_{2E1} and I_{2E2} . These are considered to belong to each donor, considering the selective excitation spectra at I_{2E1} and I_{2E2} as shown in Fig. 12. Although the spectra are complicated because of the superposition of some electronic Raman spectra, it is obvious that the emission intensity of I_{20}^{Al} in both spectra is relatively stronger than that of I_{20}^{Ga} . This means that the two peaks in excitation spectra of I_{20}^{Al} belong to the excited states of I_{20}^{Al} . Similar results are obtained on I_{20}^{Ga} . These may correspond to the vibronic or rotational levels of $I_{2\beta}$, as considered on $I_{2\alpha}$ excited levels of I_{20} .¹⁸⁻²⁰

Excited states of I_3 are more complicated than those of I_2 . It is known, from the PLE spectra on I_{3s} and I_{3w} , that the excited levels of I_{3s} are similar to those of I_{3w} and that the excited levels of I_3 states include those of I_{20} of corresponding donor species. This fact might mean that the emissions of I_3 occur at the same center

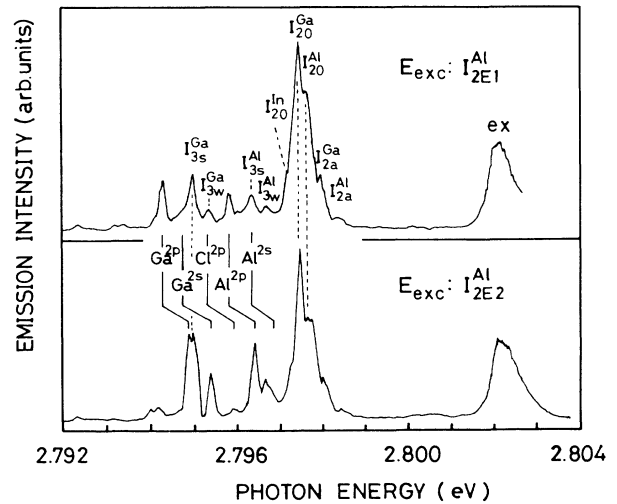


FIG. 12. Selective photoluminescence spectra. E_{exc} means the excitation energy. Some electronic Raman lines overlap with the donor-bound-exciton emission lines. The peak energy of the electronic Raman lines shift as illustrated by solid lines through the change of the excitation energy. Note that the emission intensities of I_{20}^{Al} are relatively high compared with the spectrum shown in Fig. 2.

as I_2 emissions of the corresponding donor. If the emissions of I_2 and I_3 occur at different centers, energy transfer from the I_2 center to the I_3 center should be needed. Such an energy transfer is more unlikely to occur on the purer crystals. This is contradictory to the experimental fact that the emission intensities of I_3 lines become relatively stronger with the increase of the specimen purity as shown in Fig. 10.

This deduction mentioned above is one of the possible speculations. More-detailed experimental and theoretical studies are required to understand the excited levels of I_3 and also to make the situation concerning the origin of I_3 emissions clearer.

ACKNOWLEDGMENTS

This work was supported by a Grant-in-Aid for Fundamental Scientific Research from the Ministry of Education (Grants No. 5935001 and No. 5975003). The authors are grateful to Professor K. Igaki for supporting this work and to Mr. T. Yoshida for preparing high-purity ZnSe single crystals. The authors would like to thank Professor T. Goto in the department of Physics of Tohoku University, and Professor Y. Nishina, Professor N. Kuroda, and Professor A. Kasuya at Research Institute for Iron, Steel and Other Metals, Tohoku University for their fruitful discussions.

-
- ¹M. Isshiki, T. Yoshida, T. Tomizono, S. Satoh, and K. Igaki, *J. Cryst. Growth* **73**, 221 (1985).
²M. Isshiki, T. Yoshida, K. Igaki, W. Uchida, and S. Suto, *J. Cryst. Growth* **72**, 162 (1985).
³M. Isshiki, T. Tomizono, Y. Yoshida, T. Okawa, and K. Igaki, *Jpn. J. Inst. Metals* **48**, 1176 (1984).
⁴J. L. Merz, H. Kukimoto, K. Nassau, and J. W. Shiever, *Phys. Rev. B* **6**, 545 (1972).
⁵P. J. Dean, D. C. Herbert, C. J. Werkhoven, B. J. Fitzpatrick, and R. N. Bhargava, *Phys. Rev. B* **23**, 4888 (1981).
⁶G. F. Neumark, *Phys. Rev. B* **29**, 1050 (1984).
⁷K. Igaki and S. Satoh, *Japan. J. Appl. Phys.* **18**, 1965 (1979).
⁸X. Huang and K. Igaki, *J. Cryst. Growth*, **78**, 24 (1986).
⁹S. Satoh and K. Igaki, *Jpn. J. Appl. Phys.* **20**, 1889 (1981).
¹⁰A. Kasuya, Y. Nishina, and T. Goto, *J. Phys. Soc. Jpn.* **51**, 922 (1982).
¹¹S. M. Huang, Y. Nozue, and K. Igaki, *Jpn. J. Appl. Phys.* **22**, L420 (1983).
¹²S. Permogorov, *Excitons*, edited by E. I. Rashba and M. D. Sturge (North-Holland, Amsterdam, 1982), p. 183.
¹³T. Ohshima, E. Otsuka, T. Yoshida, M. Isshiki, and K. Igaki, *Jpn. J. Appl. Phys.* **23**, L382 (1984).
¹⁴G. F. Neumark, S. P. Herko, T. F. McGee III, and B. J. Fitzpatrick, *Phys. Rev. Lett.* **53**, 604 (1984).
¹⁵T. Ohshima, E. Otsuka, T. Yoshida, M. Isshiki, and K. Igaki, in *Proceedings of the 17th International Conference on the Physics of Semiconductors*, edited by J. D. Chadi and W. A. Harrison (Springer-Verlag, New York, 1985), p. 1313.
¹⁶D. G. Thomas, J. J. Hopfield, and C. J. Frosch, *Phys. Rev. Lett.* **15**, 857 (1965).
¹⁷B. Segall and D. T. F. Marple, *Physics and Chemistry of II-VI Compounds*, edited by M. Aven and J. S. Prener (Wiley-Interscience, New York, 1967), p. 335.
¹⁸W. Ruhle and W. Klingenstein, *Phys. Rev. B* **18**, 7011 (1978).
¹⁹R. Romestain and N. Magnea, *Solid State Commun.* **32**, 1201 (1979).
²⁰P. J. Dean, D. C. Herbert, and A. M. Lahee, *Proceedings of the 15th International Conference on the Physics of Semiconductors*, Kyoto, 1980 [*J. Phys. Soc. Jpn.* **49**, Suppl. A, 185 (1980)].